www.ricuc.cl
DOI: 10.7764/RIC.00104.21

Revista Ingeniería de Construcción RIC
Vol 39 Nº2 2024
ISSN: 0718-5073

ENGLISH VERSION

Seismic performance of a multipurpose hall building using nonlinear static analysis

Desempeño sísmico de un edificio de sala multiusos mediante el análisis estático no lineal

*Curo, C. * [1] https://orcid.org/0000-0001-9841-4073;*
Ruffrán, A.. https://orcid.org/0000-0002-5321-8500¸*
*Ruiz–Pico, A.**. https://orcid.org/0000-0003-2638-0593*

* Universidad Católica Santo Toribio de Mogrovejo, Chiclayo-Perú
**Universidad Tecnológica del Perú, Chiclayo-Perú

Fecha de Recepción: 05/07/2023
Fecha de Aceptación: 01/07/2024
Fecha de Publicación: 01/08/2024
PAG:174-199

Abstract
The nonlinear static analysis method has facilitated models that are closer to the structural response for strong seismic movements. Therefore, a seismic performance evaluation of a multi-purpose hall building located in a national public university in Chiclayo, Peru, was developed, applying the nonlinear static analysis. This building comprises two similar modules, each with 3 levels and irregular plans. The building's structural system consists of load-bearing walls. It was constructed in 2010 and designed according to E.030 (the Peruvian seismic-resistant standard) and Peru's seismic microzonation. For practical purposes, considering the symmetry of the overall structure, one of the modules was evaluated using nonlinear methods capable of simulating the effect of earthquakes. This development included applying a linear analysis to establish the response spectra and, based on that, performing the nonlinear Pushover analysis. Based on the results, the performance in both directions was determined, considering the performance levels of HAZUS and VISION 2000. The results show that the building has a performance of "Life Safety" and "Near Collapse" in the X and Y directions, respectively. Additionally, the drifts show a close relationship with the performance data, as HAZUS demonstrates that the drifts in the Y direction are not favorable. Therefore, it was determined that structural reinforcement of the building is necessary to improve its unfavorable behavior.

Keywords: *Nonlinear pushover analysis; seismic performance; structural reinforcement.*

Resumen
El método de análisis estático no lineal ha facilitado modelos más cercanos a la respuesta estructural para fuertes movimientos sísmicos. Por lo tanto, se desarrolló una evaluación del desempeño sísmico de un edificio de sala multiusos ubicado en una universidad nacional pública de Chiclayo-Perú, aplicando el análisis estático no lineal, la cual contiene dos módulos semejantes de 3 niveles c/u con plantas irregulares. El sistema estructural de la edificación es de muros portantes. Fue construida en el año 2010 y fue diseñada de acuerdo a la E.030 (Norma sismo resistente peruana) y con la microzonificación sísmica de Perú. Para efectos prácticos, tomando en consideración la simetría de la estructura global, se evaluó uno de los módulos utilizando métodos no lineales que puedan simular el efecto de sismos. Este desarrollo incluía la aplicación de un análisis lineal para establecer los espectros de respuesta y a partir de ello ejecutar el análisis no lineal Pushover. En base a los resultados, se determinó el desempeño en las dos direcciones, tomando en cuenta los niveles de desempeño de la HAZUS y VISION 2000. Los resultados muestran que la edificación tiene un desempeño de "Seguridad de vida " y "Cerca al colapso " en la dirección X y Y respectivamente; además de ello, las derivas muestran una estrecha relación con los datos de desempeño, pues HAZUS demuestra que las derivas en Y no son favorables; por lo tanto, se determinó que es necesario que se ejecute un reforzamiento estructural de la edificación para mejorar el comportamiento desfavorable.

Palabras clave: Análisis estático no lineal; desempeño sísmico; reforzamiento estructural.

[1] ***Corresponding author:***
Universidad Católica Santo Toribio de Mogrovejo, Chiclayo-PERÚ
Corresponding author: carlos4curo@gmail.com

Revista Ingeniería de Construcción RIC
Vol 39 Nº2 2024
ISSN: 0718-5073

1. Introduction

Under the influence of earthquakes, reinforced concrete structures shift and deform, leading to failures of varying magnitudes as part of their performance (Jameel et al., 2013). The analysis of the performance of buildings during an earthquake is fundamental in contemporary engineering calculations (Castañeda and Mieles, 2017). The seismic behavior of structures depends on the type of soil on which they are built, their geometry, mechanical and dynamic properties, as well as soil-structure interaction (Núñez et al., 2021). Additionally, factors such as construction quality and location are vital. This latter factor is critical for the building being evaluated, situated in the "Pacific Ring of Fire," an area where 90% of the world's earthquakes occur (Gonzales et al., 2020). Countries in this belt have a high probability of experiencing high-intensity earthquakes due to the events not having released all their energy (Llontop, 2023).

The propagation of seismic waves induces vibrations that are transmitted from the foundation to the structure (Núñez et al., 2021). Therefore, it is crucial that the seismic design and evaluation of structures consider local site effects (Wang and Zhang, 2021). Seismic microzonation helps reduce risk and establishes areas with similar seismic behavior, specifying earthquake-resistant design requirements (Núñez et al., 2021). However, the building under study, located at the National University Pedro Ruiz Gallo, and 10 years old, has not undergone a pertinent seismic evaluation. Thus, its seismic performance is uncertain. Given this problem, the need to perform a seismic performance evaluation of the building against severe earthquakes was established, in accordance with the E.030 standard, with the aim of optimizing modern structural systems and improving design guidelines for earthquakes.

To determine the structure's performance, the nonlinear static Pushover analysis was applied, simulating the real effect of an earthquake on the building (Cahuana and Ccaso, 2021). This nonlinear analysis (NLA) has made it easy to evaluate the structural behavior of buildings subjected to lateral loads, such as those caused by earthquakes (Sangucho, 2022).

During this analysis, lateral loads increase until the building collapses, forming "plastic hinges" in the structural elements (Asmat, 2016). The results of the NLA provide the capacity or Pushover curve, which relates roof displacement and base shear (Díaz et al., 2022), as well as maximum displacements, drifts, degree of damage, and failure sequence of the structural elements, which absorb the earthquake's energy (Pimiento et al., 2014).

To simulate the behavior of the evaluated structure, the ETABS software was used, entering current building data obtained from preliminary studies (Quinto and Chaverra, 2022), such as soil mechanics studies, diamond drilling, steel scanning, and concrete carbonation testing. Additionally, the parameters established in the ASCE 41-17 standard for applying an appropriate nonlinear static analysis and the performance types established by VISION 2000 and HAZUS, which are based on structural displacements, given the direct relationship between lateral displacements and the level of structural and non-structural damage in buildings (Díaz et al., 2022), were used as a basis.

The contribution of this article is to evaluate the seismic performance of the building and propose a reinforcement alternative. This will improve current seismic design guidelines and optimize the structure's performance. The evaluation and reinforcement will verify the feasibility of applying certain types of reinforcement, providing greater safety and resilience to the building's occupants in the face of severe seismic events (Lloclle, 2021).

Revista Ingeniería de Construcción RIC
Vol 39 Nº2 2024
ISSN: 0718-5073

2. Methodology

To perform both linear static analysis, spectral modal analysis, and nonlinear Pushover analysis, we need to gather all the existing information related to the evaluated structure (Solorzano and Tacuche, 2023). In this way, the results we obtain will be closer to reality; for this purpose, diamond core extraction tests, soil mechanics studies, steel scanning, concrete carbonation tests, and measurements to verify the dimensions of the structural elements with the plans provided by the same institution were carried out. It is from this gathered information and the respective modeling that we can apply linear analyses, thus obtaining response spectra, maximum displacements, maximum drifts, base shears, etc.; and then

apply the nonlinear static analysis, assigning nonlinear properties, inserting plastic hinges, obtaining the performance

point with ASCE 41-17 and its performance level with VISION 2000 - HAZUS, to finally determine a viable reinforcement option that could benefit the performance of the evaluated structure (Argello, 2022). (Figure 1) shows the methodology used for the seismic performance evaluation of the structure.

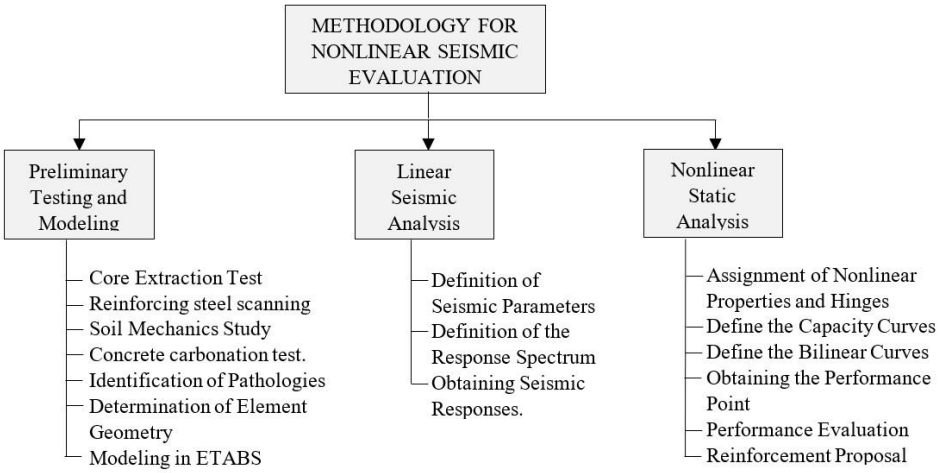

Figure 1. *Methodology for project development*

2.1. Preliminary tests and modeling in etabs

2.1.1 Core Extraction Test

For obtaining the core samples, the Peruvian technical standard NTP 339.059 was followed, which establishes the process for acquiring and testing concrete cores and determining their compressive strength (Peruana NT, 2011). This test is carried out due to the uncertainty about the current strength of the concrete (Jinez and Huarachi, 2023). Protocols such as the use of metal detectors, a minimum drilling depth of 12 cm, measuring and weighing of cores, visual verification of porosity and cracks, cutting and drying, and subsequent compression testing were applied. A total of 18 core samples were taken (9 for columns and 9 for beams), obtaining an average f'c per level, and the drilled areas were repaired

2.1.2 Reinforcement Steel Scanning

The test was based on the standard BS 1881-204, which provides recommendations for conducting the steel scan test, specifying the thickness of the cover, the diameters of the steel bars, and the location of the reinforcement bars through a scan of the concrete surface. The reinforcing steel scan test was performed with the Proceq D-tect 150 SV Scanner for 03 columns, 03 beams, and 03 concrete walls, obtaining the diameter, location, and spacing of each

of the steels (Institution, 1988).

2.1.3 Soil Mechanics Study

This test involved exploration, field evaluation, and laboratory testing, as well as the application of geotechnical engineering (Edificaciones E.050, 2018), all with the aim of determining the type of soil of the building (Cueva and Huamanchumo, 2022), based on the Peruvian technical standards E.060, E.030, and E.050. A total of 03 test pits were dug to depths of 3 meters around the building to be evaluated in order to determine the soil type according to (Table 2) of Standard E.030 and for the selection of accelerograms in case a nonlinear time history analysis is to be performed later.

2.1.4 Concrete Carbonation Test

For the execution of the test, the procedures outlined in the ASTM D-4262 standard were used to obtain the pH of the concrete. Its execution required a pH meter and a mixture of 75 grams of distilled water and 10 grams of pulverized concrete powder; a total of 4 mixtures were acquired for two selected concrete cores (ASTM, 1999).

2.1.5 Identification of Pathologies

To carry out this process, no established standard was considered, but rather a basic study which consisted of periodic visits to identify, through visual inspection, pathologies such as cracks, fissures, efflorescence, etc. (Murillo, 2022).

2.1.6 Determination of Structural Element Geometry

In order to determine the geometry of the structural elements for the modeling of the building, the elements were measured in the field and the results obtained were verified against the plans provided by the university; according to (Marín, 2022), this method also allows for obtaining the architectural distribution of the structure.

2.1.7 Building Modeling

ETABS, a software for structural analysis, was used for the modeling. The properties of the current concrete, the properties of the reinforcing steel, the loads, rigid diaphragms, rigid arms, previously measured sections, and others were entered into the software. This was done to obtain the modal results and apply the linear and nonlinear analyses.

2.2 Linear Static and Modal Spectral Analysis

The static analysis simulates seismic loads through a set of forces applied at the center of mass of each level of the building (Cumpa and Quispe, 2019), and the spectral modal analysis considers the design spectra to calculate the structure's responses. Through these two analyses, the following responses can be obtained: base shear, irregularities, maximum displacements, maximum drifts, etc. (Edificaciones E.030, 2018). To perform both analyses, the seismic parameters were established in both directions of analysis; thus, the response spectra were obtained: Z, zone factor; U, use factor; S, soil factor; C, seismic amplification factor; and R, reduction coefficient.

2.3 Nonlinear Pushover Analysis

The nonlinear Pushover analysis is a method based on applying lateral loads to a structure with small monotonic increments until collapse (Condori and Vilca, 2022). Its primary objective is to obtain the capacity curve (Ayala and Tolentino, 2021), which relates the base shear of a building and the displacement at the top floor under seismic demand. Additionally, this analysis allows identifying substantial alterations in the behavior of each element (ASCE 41-17, 2017). This analysis will be applied using ETABS software and involves:

Revista Ingeniería de Construcción RIC
Vol 39 Nº2 2024
ISSN: 0718-5073

- Application of nonlinear properties of materials: The Mander constitutive model for reinforced concrete and the Park model for reinforcing steel were considered.
- Application of plastic hinges to structural elements: These hinges will be placed at 10% and 90% of the elements due to the concentration of stresses in those areas during an earthquake.
- Obtaining the bilinear curve: To determine the performance of the building, it is necessary to establish the performance ranges. For this, SEAOC introduces established processes that involve obtaining a bilinear curve, which includes a linear range and a plastic range where the seismic behavior ranges of the structure will be found.
- Performance point: This point represents the maximum displacement of a structure under seismic demand, and to determine its value, the coefficient method based on ASCE 41-17 was applied, which provides the procedures for its calculation:
i. Selection of "Co": Modification factor to relate the spectral displacement of a single degree of freedom (SDOF) system with the roof displacement of a multi-degree of freedom (MDOF) system (Figure 2).

	Shear Buildings[a]		Other Buildings
Number of Stories	Triangular Load Pattern (1.1, 1.2, 1.3)	Uniform Load Pattern (2.1)	Any Load Pattern
1	1.0	1.0	1.0
2	1.2	1.15	1.2
3	1.2	1.2	1.3
5	1.3	1.2	1.4
10+	1.3	1.2	1.5

Note: Linear interpolation shall be used to calculate intermediate values.
[a] Buildings in which, for all stories, story drift decreases with increasing height.

Figure 2. *Values of "Co" according to ASCE 41-17*

ii. Fundamental period of vibration (Ti): The time it takes for the structure to complete one vibration.
iii. Pseudo acceleration Sa (g): This value is obtained by multiplying the ZUCS/R from (Table 11) by the reduction coefficient R.
iv. Factor Cm: The value of the effective mass, which depends on the type of building and the number of floors, as shown in (Figure 3).

No. of Stories	Concrete Moment Frame	Concrete Shear Wall	Concrete Pier-Spandrel	Steel Moment Frame	Steel Concentrically Braced Frame	Steel Eccentrically Braced Frame	Other
1–2	1.0	1.0	1.0	1.0	1.0	1.0	1.0
3 or more	0.9	0.8	0.8	0.9	0.9	0.9	1.0

Note: C_m shall be taken as 1.0 if the fundamental period, T, in the direction of response under consideration is greater than 1.0 s.

Figure 3. *Effective Mass Values (Cm)*

Revista Ingeniería de Construcción RIC
Vol 39 Nº2 2024
ISSN: 0718-5073

v. Seismic Weight W: 100% of the dead load and 50% of the live load were considered, as per the E.030 standard for essential buildings.
vi. Yield Shear Vy: The elastic limit of the building calculated using the NSP results for the idealized nonlinear force-displacement curve.
vii. Ustrng: Ratio between the elastic strength demand and the yield limit; its value is obtained from the following formula (Equation 1):

$$Ustrng = \frac{Sa}{Vy/W} Cm \quad (1)$$

Where:

Sa: Pseudo Acceleration
Vy: Yield Shear
W: Seismic Weight

viii. Site factor (a): The ASCE 41-17 standard provides "a" values depending on the type of soil of the building. A similarity was drawn between the type of soil obtained using the E.030 standard and the soil types provided by ASCE 41-17 (A, B, D, E, and F).
ix. Ki: Elastic lateral stiffness: obtained through the capacity curve, dividing the shear by the displacement at the elastic range limit.
x. Ke: Effective lateral stiffness: obtained through the bilinear curve, dividing the shear by the displacement at the elastic range limit.
xi. Effective fundamental period (Te): formula 7-27 of the ASCE 41-17 standard (Equation 2).
xii.

$$Te = Ti\sqrt{\frac{Ki}{Ke}} \quad (2)$$

Where:
Ti: Fundamental Vibration Period
Ki: Elastic Lateral Stiffness
Ke: Effective Lateral Stiffness

xiii. Obtaining the coefficient C1: Modification factor to relate the expected maximum inelastic displacements to the displacements calculated for the calculated linear elastic response (Equation 3).

$$C_1 = 1 + \frac{u_{strength} - 1}{aT_e{}^2} \quad (3)$$

Revista Ingeniería de Construcción RIC
Vol 39 Nº2 2024
ISSN: 0718-5073

Where:
a: Site Factor
Te: Effective Fundamental Period
Ustrength: Ratio of Elastic Demand to Elastic Limit
xiv. Obtaining the coefficient C2: Modification factor to represent the cyclic stiffness degradation and strength deterioration (Equation 4).

$$C_2 = 1 + \frac{1}{800}\left(\frac{u_{strength} - 1}{Te}\right)^2 \quad (4)$$

Where:
Te: Effective Fundamental Period
Ustrength: Ratio of Elastic Demand to Elastic Limit

xvi. Performance point: Maximum displacement of the structure (Equation 5).

$$\delta_t = C_0 C_1 C_2 S_a \frac{T_e^2}{4\pi^2} g \quad (5)$$

Where:
Te: Effective Fundamental Period
g: Gravity
C0 C1 C2: Modification Factors
Sa: Pseudo Acceleration
Ustrength: Ratio of Elastic Demand to Elastic Limit

3. Results

3.1 Preliminary tests and modeling

3.1.1 Core Extraction Test

The maximum and minimum average values of the concrete strength obtained were 142 kg/cm² and 88.5 kg/cm², respectively, which indicates low compressive strength of the columns and beams of the multi-purpose hall building, considering that the f'c used for its design was 210 kg/cm ² (Table 1).

Revista Ingeniería de Construcción RIC
Vol 39 Nº2 2024
ISSN: 0718-5073

Table 1. *Average Compressive Strength (f'c) of Columns and Beamsvalidity of the questionnaire*

Floor Nº	STRUCTURAL ELEMENT	AVERAGE CORRECTED f'c (kg/cm²)
1st	Column	142
	Beam	142
2nd	Column	136
	Beam	130
3rd	Column	116
	Beam	88.5

3.1.2 Reinforcement Steel Scanning

(Table 2) (Table 3) and (Table 4) show that the predominant steel diameter in both beams and columns is 3/4" and 3/8" for longitudinal and transverse reinforcement, respectively; for concrete walls, the predominant steel diameter is 3/8 ".

Table 2. *Reinforcement Steel Distribution in Concrete Walls*

Steel/Elements		Wall 1	Wall 2	Wall 3
Separation (m)		0.225	0.225	0.225
Cover (cm)		4.0	5.0	6.0
Ø Steel (in)	Long.	3/8	3/8	3/8
	Transv.	3/8	3/8	3/8

Table 3. *Reinforcement Steel Distribution in Columns*

Steel/Elements		Col.1 - (30x50)	Col.2 - (30x60)	Co.3 - (30x45)
N°. of Longitudinal Bars Detected	Side N°1	2.0	2.0	2.0
	Side N°2	2.0	2.0	2.0
	Side N°3	1.0	2.0	1.0
Number of Stirrups		18	18	22
Cover (cm)		6.0	5.0	5.0
Ø Steel (in)	Long.	3/4	3/4	3/4
	Trans.	3/8	3/8	3/8

Revista Ingeniería de Construcción RIC
Vol 39 Nº2 2024
ISSN: 0718-5073

Table 4. *Reinforcement Steel Distribution in Beams*

Steel/Elements		Beam 1 (30x40)	Beam 2 (30x50)	Beam 3 (15x40)
N°. of Longitudinal Bars Detected	Side N°1	1.0	2.0	1.0
	Side N°2	2.0	2.0	2.0
	Side N°3	2.0	2.0	2.0
Number of Stirrups		30	37	22
Cover (cm)		6.0	6.0	5.0
Ø Steel (in)	Long.	3/4	3/4	1/2 y 3/8
	Trans.	3/8	3/8	1/4

3.1.3 Soil mechanics study

From the three test pits obtained, it was determined that the soil type of the building is S3 (Table 5), which means soft soil with wave propagation speeds of less than or equal to 180 m/s, predominantly composed of low plasticity clay with sand.

Table 5. *Soil Mechanics Study Results*

SOIL PROFILE	S3 (Soils floors)
FOUNDATION TYPE	Superficial
FOUNDATION DEPTH	1.50 meters
PREDOMINANT MATERIAL	CL (Low plasticity clay with sand).
AVERAGE ALLOWABLE LOAD CAPACITY	1.02 kg/cm2
SECURITY FACTOR	3

3.1.4 Concrete carbonation test

(Graph 1) shows that the tested samples have pH values greater than 12, indicating that there are no signs of carbonation in the concrete.

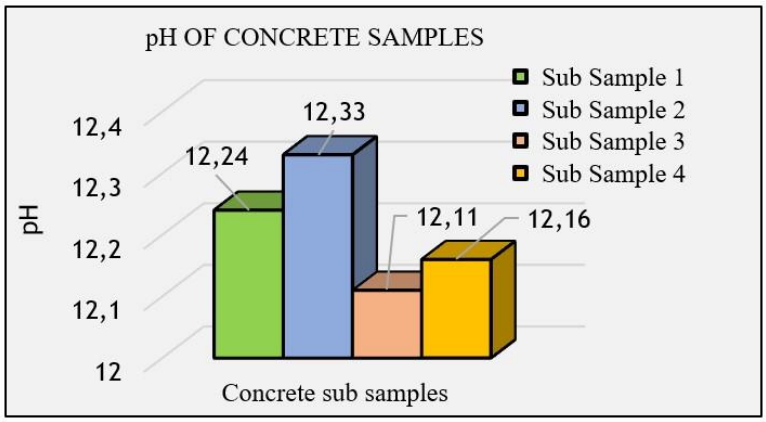

Graph 1. *Concrete Carbonation Test Results*

Revista Ingeniería de Construcción RIC
Vol 39 Nº2 2024
ISSN: 0718-5073

3.1.5 Identification of pathologies

The following pathologies were evidenced: In physical pathologies, the most common indicator was moisture, present at the various peripheral edges of the building; within mechanical pathologies, the most common indicators were cracks and fissures with lengths of up to 20 and 80 centimeters, respectively; finally, in chemical pathologies, the most common indicator was efflorescence, present in various areas around the perimeter of the structure. All this indicates a lack of maintenance of the building.

3.1.6 Identification of pathologies

The dimensions of the structural elements presented in (Table 6) match the dimensions specified in the structural plans provided by the institution.

Table 6. *Dimensions of Structural Elements*

Denomination	Dimensions
Column COL Nº1	0.30 x 0.45 m
Column COL Nº2	0.30 x 0.50 m
Column COL Nº3	0.30 x 0.60 m
Beam VX	0.30 x 0.45 m
Beam VY	0.30 x 0.50 m
Beam VE	0.30 x 0.35 m
Beam VS	0.30 x 0.40 m
Lightened slab	e = 0.25 m
Concrete walls	e= 0.20 m

3.1.7 Identification of pathologies

For the modeling, the information resulting from the tests carried out was considered, as well as the E.020 and E.060 standards for the specific weights and the modules of elasticity (Table 7).

Table 7. *Properties of Materials*

Materials	Properties
Reinforced concrete	Unit Weight 2400 kg/m3 Module of Poisson u=0.15
Reinforcing steel	yield strength fy=4200 kg/cm2 Unit weight 7850 kg/m3 Poisson's modulus 2000000 kg/cm2

Subsequently, dead and live loads were assigned, referencing the E.020 standard; for the perimeter walls, a manual measurement was performed to obtain their distributed load See (See (Table 8) and (Table 9).

Table 8. *Dead Loads*

Dead loads	
Lightened slabe=25cm	0.350 Ton/m^2
Non-bearing wallsNº1	0.658 Ton/m
Non-bearing walls Nº1	0.365 Ton/m
Interior Partition Equiv.	0.150 Ton/m^2
Finishes	0.100 Ton/m^2
Alféizar	0.162 Ton/m

Table 9. *Live Loads*

Revista Ingeniería de Construcción RIC
Vol 39 Nº2 2024
ISSN: 0718-5073

Live Loads	
Losa- Classroom	0.250 Ton/m^2
Losa- Corridor	0.400 Ton/m^2
Losa- Roof	0.100 Ton/m^2

With the obtained information, the building was modeled (Figure 4), considering three rigid diaphragms, a seismic weight of 100% DL (Dead Load) and 50% LL (Live Load) according to E.030 for essential buildings; "release" and rigid arms were applied to the building for the moments; this resulted in a total seismic weight of approximately 814 tons.

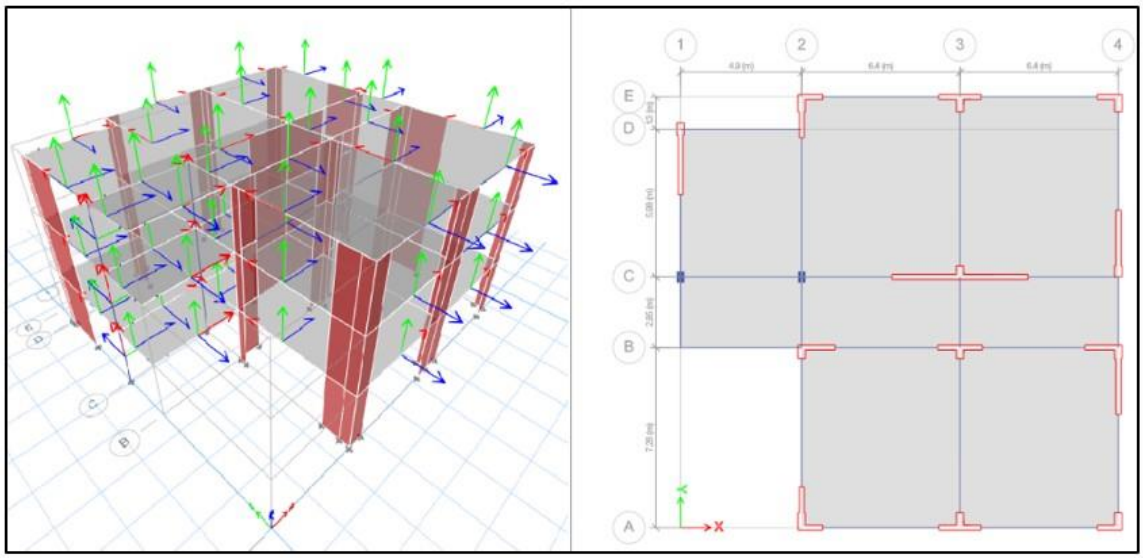

Figure 4. *Building Modeling in ETABS Software*

With the building already modeled, the modal results were obtained (Table 10). Twelve vibration modes were obtained with a sum of effective masses of at least 90%, complying with Article 29.1.2 of the E.030 standard, and a maximum fundamental period of vibration of 0.279 seconds.

Table 10. *Modal Results*

Vibration modes				
Modes	Period "I" (seg)	Participatory Mass		
		Ux	Uy	Rz
1	0.279	0.000	0.515	0.223
2	0.253	0.713	0.011	0.017
3	0.220	0.028	0.222	0.502

Revista Ingeniería de Construcción RIC
Vol 39 Nº2 2024
ISSN: 0718-5073

3.2 Linear static and spectral modal analysis

From the tests conducted, the modal results of the structural modeling, and the information present in the E.030 standard, the seismic parameters, the fundamental period of vibration, the ZUCS/R coefficient, etc., were obtained (See (Table 11)), which are fundamental data for performing the linear static analysis and the modal spectral dynamic analysis.

Table 11. *Seismic Parameters*

SEISMIC PARAMETERS		X	Y
Z – Zone Factor	ZONE 4	0.45	0.45
U – Importance coefficient	Type: A	1.50	1.50
S – Soil Factor	Type S3	1.10	1.10
Tp - Predominant period		1.00	1.00
TL – Local Period		1.60	1.60
T – Fundamental Period		0.25	0.28
C – Seismic amplification		2.50	2.50
Ro – Reduction coefficient		6.00	6.00
Ia – Height irregularity		1.00	1.00
Ip – Floor irregularity		0.90	0.75
Irregularity Verification		Irregular	Irregular
R – Reduction coefficient		5.40	4.50
Coefficient $ZUCS/R$		0.34	0.41
Relation. C/R		0.42	0.42
Verification Article 28.2.2		Complies	Complies
Displacement factor		5.10	5.10
Kx Seismic force distribution factor		1.00	1.00

In the ETABS software, the load patterns for the linear static analysis were inserted, considering a ZUCS/R coefficient of 0.34 for the X-axis and 0.41 for the Y-axis, and a seismic force distribution factor of 1 for both directions. Additionally, two load cases were considered for the modal spectral dynamic analysis by inserting the response spectra
developed with the seismic parameters from (Table 11).

Prior to this definitive linear analysis, a preliminary one was executed, considering irregularity factors of 1 in plan and elevation; however, after executing the analyses, it was concluded that the structure presents both types of irregularity. The most critical ones can be seen in (Table 12) and (Table 13).

Table 12. *Mass or Weight Irregularity*

MASS OR WEIGHT IRREGULARITY				
Floor	Weight	Greater than		Verification
		Down	Up	>1.5
3	19.90	0.67	-	Accomplish
2	29.86	1.00	1.50	No accomplish
1	29.86	-	1.00	Accomplish

Revista Ingeniería de Construcción RIC
Vol 39 Nº2 2024
ISSN: 0718-5073

Table 13. *Torsional Irregularity in Y*

Y-Y TORSIONAL IRREGULARITY			
Floor	Item	Ratio	Δmax > 1.3 Prom
Floor 3	Diaph D3 Y	1.388	IRREGULAR
Floor 2	Diaph D2 Y	1.37	IRREGULAR
Floor 1	Diaph D1 Y	1.342	IRREGULAR

Subsequently, the linear analyses were re-executed with the irregularity coefficients in plan and elevation in both directions, obtaining maximum base shears of 268 tons and 322 tons in the X and Y directions, respectively, as presented in (Table 14) and (Table 15).

Table 14. *Base Shears from Linear Static Analysis (LSA)*

STATIC BASAL SHEAR		
BASE SHEAR X-X	268.3961	Ton
BASE SHEAR Y-Y	322.0754	Ton

Table 15. *Base Shears from Linear Dynamic Analysis (LDA)*

DYNAMIC BASE SHEAR		
BASE SHEAR X-X	202.0166	Ton
BASE SHEAR Y-Y	202.3302	Ton

The maximum displacements were also obtained, as presented in (Tables 16) and (Table 17), calculated by multiplying the displacements from the linear analysis by 0.85R for irregular structures according to E.030.

Table 16. *Maximum Displacements from LDA*

Linear Dynamic Analysis				board verification
Floor	Axis	Maximum displacement	Displ. (cm)	< 2cm
3	X	0.042764	4.2764	No Accomplish
2	X	0.024545	2.4545	No Accomplish
1	X	0.007991	0.7991	Accomplish
3	Y	0.057857	5.7857	No Accomplish
2	Y	0.032657	3.2657	No Accomplish
1	Y	0.010487	1.0487	Accomplish

Table 17. *Maximum Displacements from LSA*

Linear Static Analysis				board verification
Floor	Axis	Maximum displacement	Displ. (cm)	< 2cm
3	X	0.045294	4.5294	No Accomplish
2	X	0.026207	2.6207	No Accomplish
1	X	0.008744	0.8744	Accomplish
3	Y	0.051688	5.1688	No Accomplish
2	Y	0.029511	2.9511	No Accomplish
1	Y	0.009689	0.9689	Accomplish

As can be seen in (Tables 16) and (Table 17), the displacements exceed the current seismic joint of the building; therefore, the phenomenon of pounding is likely to occur in the event of rare or very rare earthquakes. Additionally, drift values were obtained, which, according to (Table 11) of the E.030 standard, should not exceed a value of 0.007 for reinforced concrete structures. However, in (Table 18), the Y-axis shows otherwise, which is not ideal for the structure.

Table 18. *Drifts from LDA*

Linear Dynamic Analysis			
Direction	N.ºFloor	Drift Inel.	<0.007
Drift X	3	0.005222	Accomplish
Drift X	2	0.004735	Accomplish
Drift X	1	0.002283	Accomplish
Drift Y	3	0.00722	No Accomplish
Drift Y	2	0.006342	Accomplish
Drift Y	1	0.002996	Accomplish

Table 19. *Drifts from LSA*

Linear Static Analysis			
Direction	N.ºFloor	Drift Inel.	<0.007
Drift X	3	0.005453	Accomplish
Drift X	2	0.00499	Accomplish
Drift X	1	0.002498	Accomplish
Drift Y	3	0.006336	Accomplish
Drift Y	2	0.005664	Accomplish
Drift Y	1	0.002768	Accomplish

3.3 Nonlinear pushover analysis

3.3.1 Assignment of nonlinear properties and plastic hinges

For the concrete, the Mander model is being considered for the stress-strain diagrams, and for the reinforcing steel, the Park model is being considered. Below, the stress-strain (Graph 2) and (Graph 3) are shown, which will be used for the evaluation.

Revista Ingeniería de Construcción RIC
Vol 39 Nº2 2024
ISSN: 0718-5073

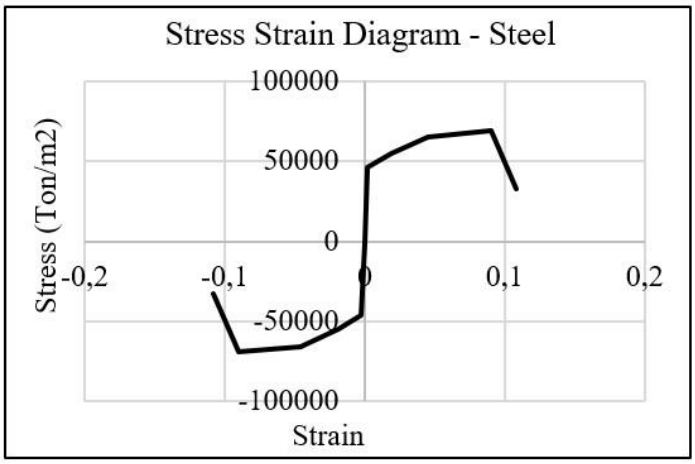

Graph 2. *Steel Stress-Strain Diagram*

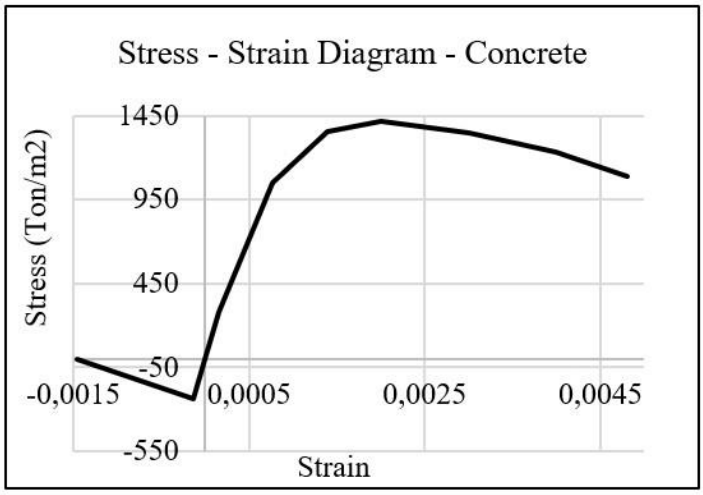

Graph 3. *Concrete Stress-Strain Diagr*

Next, the plastic hinges were placed for the columns, beams, and reinforced concrete walls, as shown in (Figure 5).

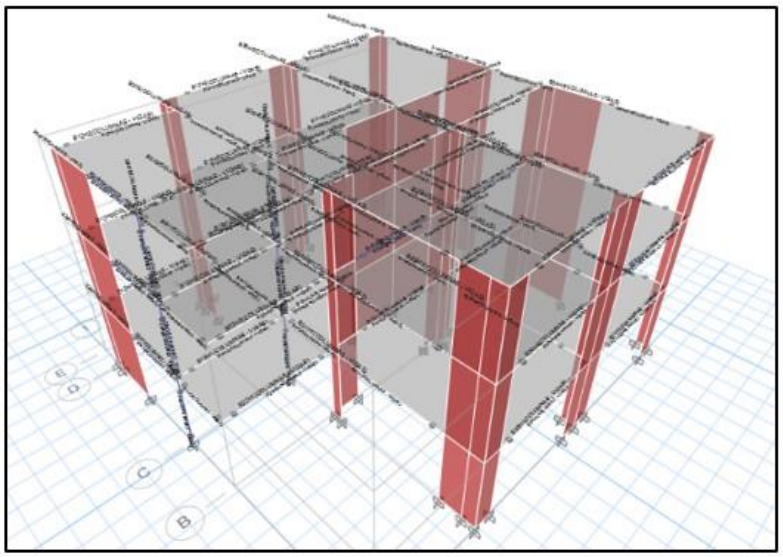

Figure 5. *Placement of Plastic Hinges on Structural Elements*

Revista Ingeniería de Construcción RIC
Vol 39 Nº2 2024
ISSN: 0718-5073

3.3.2 Obtaining the Capacity Curve and Performance Point

Prior to an earthquake, structures are subjected to their own weight and then impacted by seismic movements. For this reason, a load case called "Gravity Load" must be generated in the ETABS software, considering 100% dead load and 50% live load according to ASCE 43-17. The control point N°. 13 is chosen as it is the closest point to the center of gravity of the structure on the rooftop.

Next, load cases for the nonlinear Pushover analysis are created in both the X and Y directions, using control point N°. 13 and the mode of vibration with the longest period corresponding to each direction of analysis. Additionally, control displacements of 0.16 m and 0.15 m were considered for the X and Y axes, respectively. With the input data, a capacity curve in the X direction was obtained with a maximum shear of 501 tons, and a capacity curve in the Y direction with a maximum shear of 443 tons (see (Graph 4) and (Graph 5).

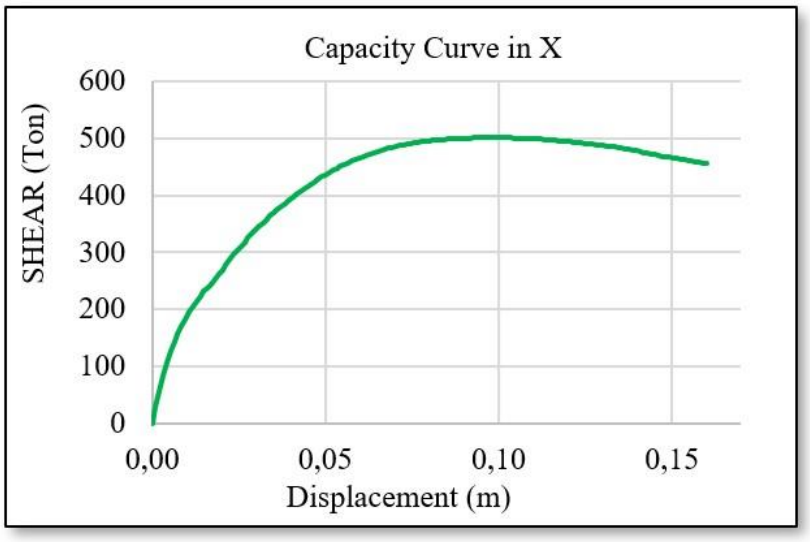

Graph 4. *Capacity Curve in the X Direction*

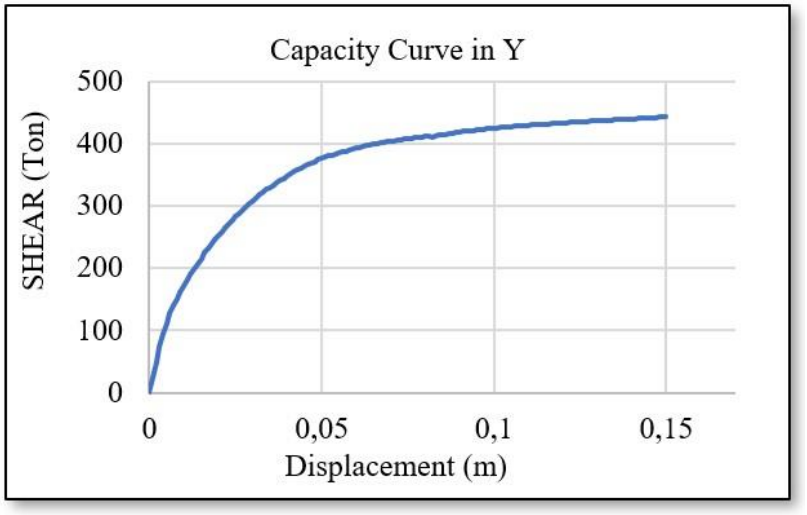

Graph 5. *Capacity Curve in the X Direction*

To determine the performance, we need the performance point and the ranges of the different behavior

Revista Ingeniería de Construcción RIC
Vol 39 Nº2 2024
ISSN: 0718-5073

levels provided by Vision2000. For this, the SEAOC method was used to develop the location of the ranges, starting by establishing the bilinear curves for the X and Y axes (see (Grap 6) and (Graph 7).

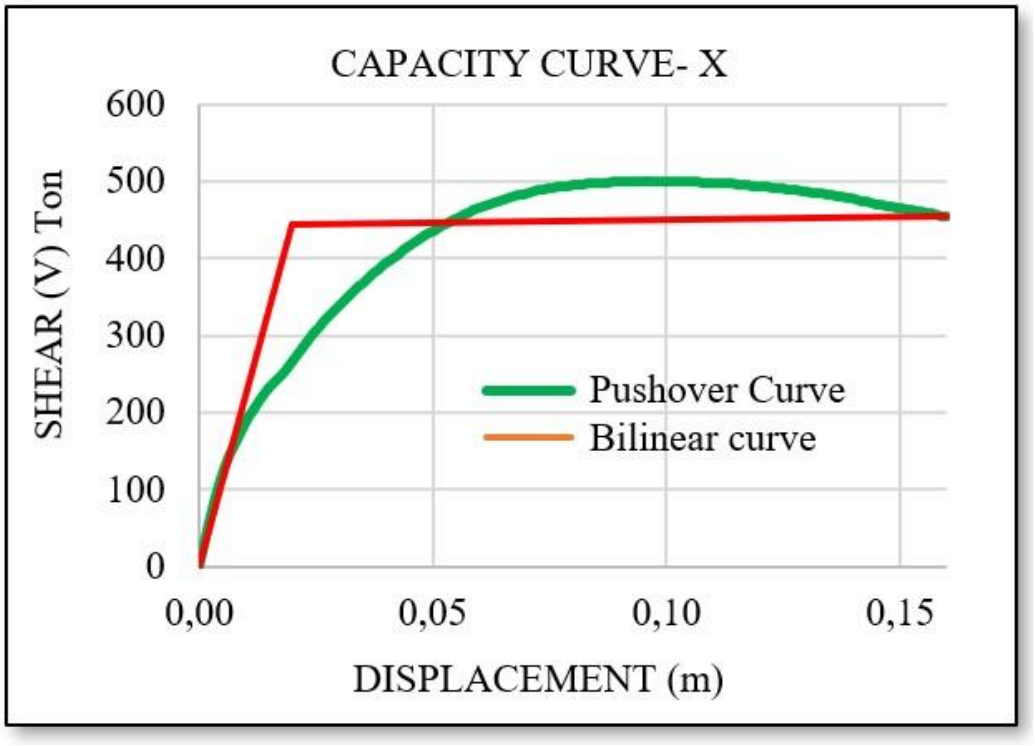

Graph 6. *Bilinear Curve in the X Direction*

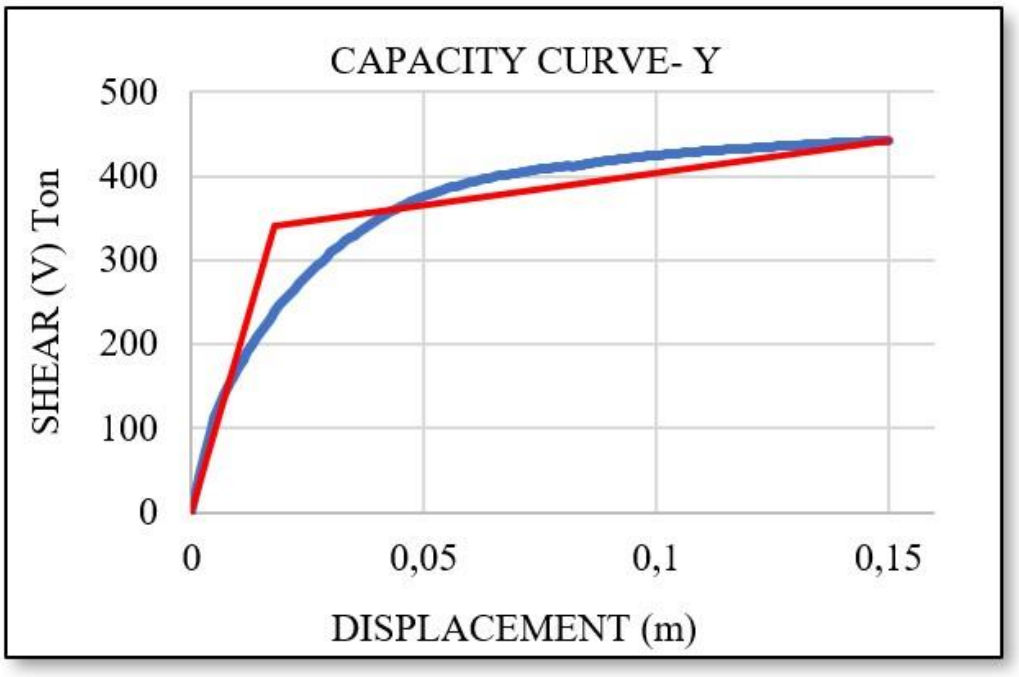

Graph 7. *Bilinear curve in the Y direction*

The bilinear curve should extend to the end of the capacity curve, and it must ensure that the two areas

formed together with the capacity curve have the same magnitude. This meets the energy principle, resulting in an elastic section and a plastic section.

The intermediate value of the bilinear curve must be calibrated to achieve the energy principle. Additionally, it is with this bilinear curve that the location of the ranges for the different performance levels can be determined. The values of the bilinear curves for the X and Y axes are shown below in (Table 20) and (Table 21).

Table 20. *Bilinear Curve for X Axis*

Bilinear Curve	
D (m)	V (Tn)
0	0
0.02	445
0.16	455.0088

Table 21. *Bilinear Curve for Y Axis*

Bilinear Curve	
D (m)	V (Tn)
0	0
0.018	340
0.150	443.174

Next, based on the values of the bilinear curve, the performance ranges were established, starting from the onset of the plastic state of the bilinear curve to its end, which should coincide with the end of the capacity curve (see (Table 22), (Table 23) and (Graph 7) and (Graph 8)).

Table 22. *X-axis performance ranges*

Operational	Δe	0.0200 m
Functional	Δe+0.3(Δp)	0.0620 m
Life Security	Δe+0.6(Δp)	0.1040 m
Close to collapse	Δe+0.8(Δp)	0.1320 m
Collapse	0.2(Δp)	0.1600 m

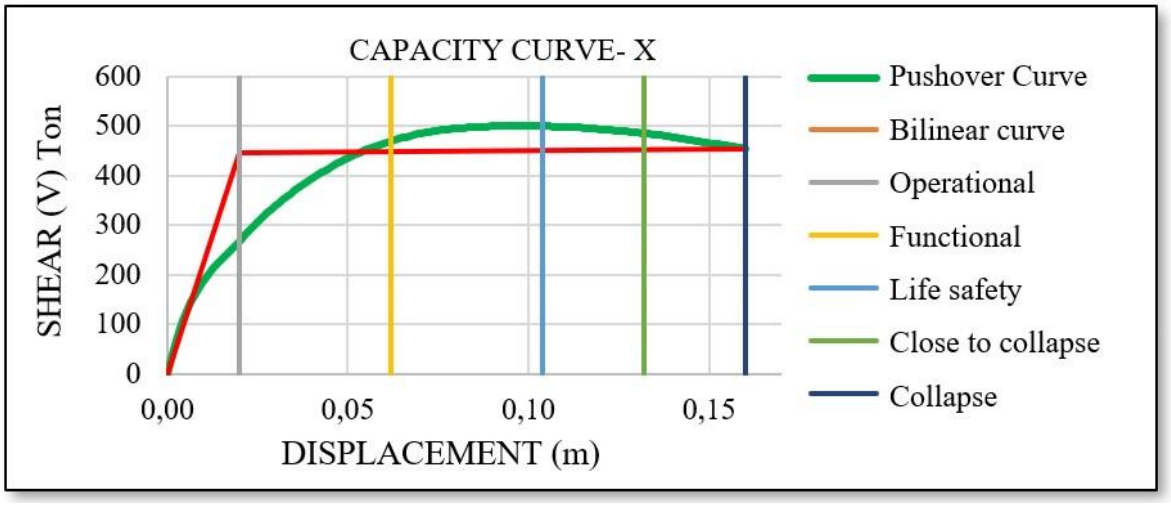

Graph 7. *Performance Ranges for X Axis*

Table 23. *Performance Ranges for Y*

Operational	Δe	0.0180 m
Functional	Δe+0.3(Δp)	0.0576 m
Life Security	Δe+0.6(Δp)	0.0972 m
Close to collapse	Δe+0.8(Δp)	0.1236 m
Collapse	0.2(Δp)	0.1500 m

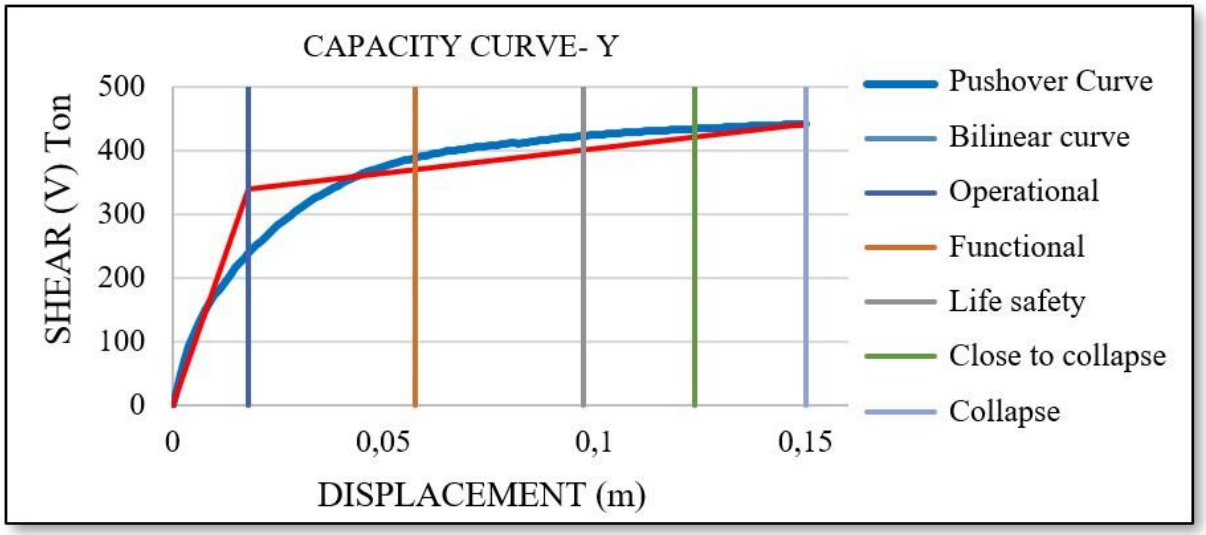

Graph 8. *Performance Ranges for Y*

Next, the performance point was calculated using the coefficient method based on the ASCE 41-17 standard. (Table 24)

- Results of the Coefficient Method

***Table 24.** Results of Coefficient Method*

	X	Y
a) Selection of Co	1.30	1.30
b) Period - ti	0.253 Seg	0.279 Seg
c) Acceleration Sa(g)	1.856	1.856
d) Factor Cm	0.8	0.8
e) Seismic weight W	813.6 Tn	813.6 Tn
f) Yield Shear	462.2 Tn	334.0 Tn
g) Ustrng	2.6142	3.6170
h) a (Site factor)	60	60
i) Ki (Ton/m)	27149.30	24950.55
j) Ke (Effective) Ton/m	13214.03	15276.55
k) Te (Seg)	0.3626	0.3566
l) Coefficient C1	1.205	1.343
m) Coefficient C2	1.025	1.067
n) Performance point	9.73 cm	10.93 cm

The results show that the X-axis achieved a performance point of 9.73 cm and the Y-axis of 10.93 cm, with base shears of 501 tons and 430 tons, respectively, obtained from the ETABS software. Based on this, the performance results are shown using the damage levels of Vision 2000 (Graph 9) and (Graph 10) and Table 5.9b of HAZUS (Figure 6).

Revista Ingeniería de Construcción RIC
Vol 39 Nº2 2024
ISSN: 0718-5073

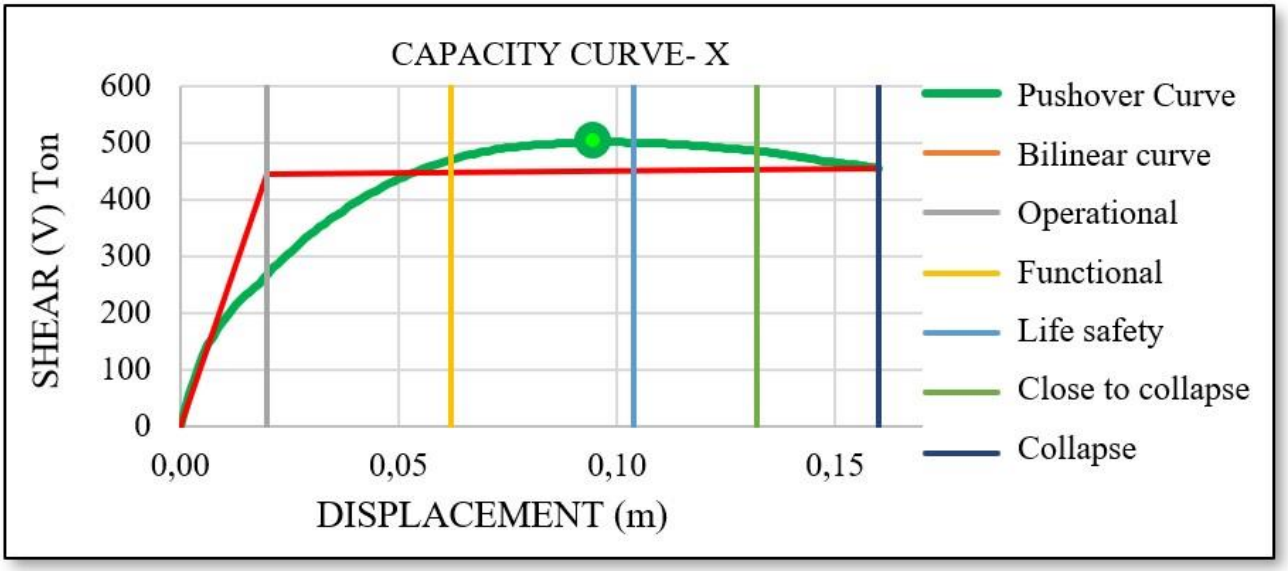

Graph 9. *Performance in X Axis*

The performance in the X-axis would fall under "life safety."

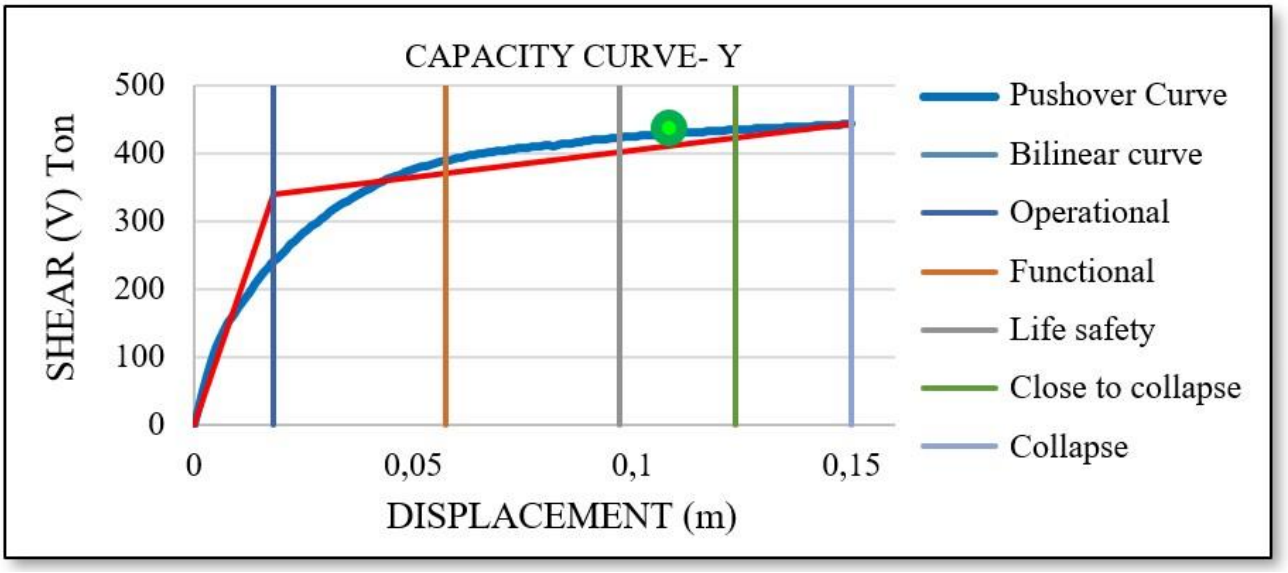

Graph 10. *Performance in Y Axis*

Revista Ingeniería de Construcción RIC
Vol 39 Nº2 2024
ISSN: 0718-5073

The performance in the Y-axis would fall under "near collapse."

Table 5.9b Structural Fragility Curve Parameters – Moderate Code Seismic Design Level

Building Properties			Interstory Drift at Threshold of Damage State			
Type	Height (inches)					
	Roof	Modal	Slight	Moderate	Extensive	Complete
C1L	240	180	0.0050	0.0087	0.0233	0.0600
C1M	600	450	0.0033	0.0058	0.0156	0.0400
C1H	1440	864	0.0025	0.0043	0.0117	0.0300
C2L	240	180	0.0040	0.0084	0.0232	0.0600
C2M	600	450	0.0027	0.0056	0.0154	0.0400
C2H	1440	864	0.0020	0.0042	0.0116	0.0300

Figure 6. *HAZUS Performance Levels*

Considering that the maximum drift in the X and Y directions obtained from the nonlinear Pushover analysis is 0.0112 and 0.1093, respectively, they would therefore fall within the "Collapse" range for the performance levels proposed by HAZUS.

4. Discussion

The concrete compressive strength and scanner tests show that the plans were not executed as specified. This demonstrates inconsistencies between the actual built structure and the design model, which can lead to failures and valuable lessons later, as occurred with many of the buildings that collapsed in the 2016 Ecuador earthquake (Castañeda and Mieles, 2017). On the other hand, regarding irregularities, the Peruvian standard E.030 establishes a series of restrictions for an essential building located in zone 4. The results obtained from this project show that the multi-purpose hall building did not meet the requirements due to irregularity in plan and elevation. This differs from the results of the 5-story structural wall building by (Eduardo, 2019); however, this situation is allowed because his building is of a common type . Moreover, the present structure does not have seismic isolation, and not all its drifts are below 0.007, as the lateral stiffness varies from one direction to another (Firoj et al., 2022). This can be solved with a proper distribution of walls, like the 10-story structural wall building by (Azabache and Briceño, 2024), who obtained maximum inelastic drifts of 0.00205 and 0.0068.

Traditional modeling in ETABS software involves a reasonable period to obtain the building's responses to nonlinear Pushover analysis; this can be linked to the project's magnitude, equipment performance, etc. (Tagle et al., 2021) shows that it is possible to optimize this procedure with simplified inelastic finite element simulation approaches in software like DINA, requiring only 54% of the computational time needed for 3D modeling of the structure.

Applying the coefficient method to obtain the maximum displacement under seismic demand shows a

base shear of 500.98 tons and a displacement of 9.72 cm in the X-axis, while in the Y-axis, the base shear is 430.698 tons and the displacement is 10.93 cm. This variability is explained by the Y direction having fewer bearing walls than the X direction, resulting in lower stiffness and ductility. Similar results were found in the study by (Firoj et al., 2022), which demonstrated the importance of a proper distribution of structural elements to resist loads in both directions. (Choque and Luque, 2019) found that their 8-story structural wall building had maximum displacements of 21.9 cm and 21.3 cm in the X and Y directions, respectively, due to its high ductility from the low presence of structural walls. In contrast, the building evaluated by Diego Villagra (Eduardo, 2019) presented maximum displacements of 1.6 cm and 1.35 cm in the X and Y directions, respectively, due to an excessive distribution of stiffening elements.

The Pushover analysis allowed determining the performances of "Life Safety" and "Near Collapse" in the X and Y directions, respectively. Studies like that of (Arumugam et al., 2022) similarly show the effectiveness of this analysis for advanced reinforced concrete structures, obtaining performance values similar to those in the present study. Additionally, in evaluating the seismic behavior of regular and irregular moment-resisting composite frames, the global yielding of the structure could be determined from the nonlinear Pushover analysis (Etli and Güneyisi, 2020). The evaluation of the Sant'Agostino church in L'Aquila by (Cennamo and Fiore, 2013) is also noteworthy. However, this only proves the method's efficiency and not a relationship of structural behaviors since each structure has a unique behavior under seismic demands. Referring to cases of the same nature, (Tello and Yacsavilca, 2023) evaluated a 5-story building, which resulted in a performance of "Moderate." Subsequently, they included dampers, resulting in a performance of "Light," which is an alternative for optimizing future structures.

5. conclusions

Through linear static and modal spectral analysis, the multi-purpose hall building exhibits maximum drifts of 0.00545 in the X direction and 0.007219 m in the Y direction, complying with the maximum limit of 0.007 for reinforced concrete buildings in the X direction, but not in the Y direction. Additionally, it is irregular in plan and elevation, experiencing critical irregularities in torsion and mass or weight.

The capacity curve of the multi-purpose hall building in the X direction shows an ultimate base shear of 455.01 tons and a displacement of 0.16 m, while the Y direction presents an ultimate shear of 443.174 tons and a displacement of 0.15 m. With this information, the target displacements could be determined. In the X direction, the target displacement is 0.0973 m with a base shear of 500.98 tons, and in the Y direction, a target displacement of 0.1093 m was obtained with a base shear of 430.698 tons.

Using the obtained performance points and following the Vision 2000 performance proposals, it was concluded that in the X direction, the performance is classified as "Life Safety," where structural and non-structural components show moderate damage but maintain a margin against collapse. Additionally, it meets the objective of standard E.030. Therefore, it is concluded that reinforcement is not necessary in the X direction, but it is required in the Y direction as its performance is classified as "Near Collapse," which coincides with the performance results obtained with HAZUS for the Y direction.

It is concluded that reinforcement is necessary in the Y direction, such as jacketing to form a wall from the columns, as proposed by engineer Blanco Blasco. This technique increases the stiffness of the structure. Moreover, if applied to a specific element to control the center of rigidity and prevent its significant displacement relative to the center of mass, the torsional irregularity could be mitigated. This procedure would be carried out using concrete with a higher compressive strength (f'c) than the original design of the structure. Additionally, the inclusion of stiffening elements through the demolition and insertion of structural components to control

Revista Ingeniería de Construcción RIC
Vol 39 Nº2 2024
ISSN: 0718-5073

displacements in the most unfavorable direction is recommended, as suggested by engineer Patricio Placencia, using concrete with a minimum compressive strength of 210 kg/cm².

7. Referencias

Argüello, C. (2022). *Análisis y diseño estructural del edificio Mushuc Runa de diez pisos en estructura metálica, mediante comparación del análisis estático lineal, modal, estático no lineal (pushover), dinámico no lineal (historia de respuesta), y diseño estructural en concordancia con el AISC 341-16, AISC 358-16, e incidencia en las condiciones actuales de la edificación [Universidad Tècnica de Ambato].*

Arumugam, V.; Keshav, L.; Achuthan, A.; Dasappa, S. (2022). *Seismic Evaluation of Advanced Reinforced Concrete Structures. Hindawi, 8.*

ASCE/SEI 41-17. (2017). *Seismic Evaluation and Retrofit of Concrete Buildings. California, USA.*

Asmat, C. (2016). *Disposiciones sísmicas de diseño y análisis en base a desempeño aplicables a edificaciones de concreto armado. Pontifica Universidad Católica del Perú.*

ASTM. (1999). *Standard Test Method for pH of Chemically Cleaned or Etched Concrete Surfaces ASTM D 4262. West Conshohocken.*

Ayala, E.; Tolentino, M. (2021). *Desempeño sísmico del pabellón "D" de la I. E. Francisco Bolognesi, mediante el análisis estático no lineal "Pushover", distrito Chilca, Huancayo, 2021 [Universidad Continental]. https://repositorio.continental.edu.pe/bitstream/20.500.12394/11451/2/IV_FIN_105_TE_Orihuela_Orihuela_2021.pdf*

Azabache, W.; Briceño, A. (2024). *Análisis sísmico lineal y diseño estructural de una vivienda multifamiliar de concreto armado de 10 niveles - Ubicado en el distrito de Trujillo [Universidad Privada Antenor Orrego]. https://repositorio.upao.edu.pe/bitstream/handle/20.500.12759/32571/REP_WILLIANS.AZABACHE_AIMAR.BRICE%c3%91O_ANALISIS.SISMICO.pdf?sequence=1&isAllowed=y*

Cahuana, M.; Ccaso, G. (2021). *Desempeño sísmico aplicando el análisis estático no lineal (Pushover) del módulo III de la comisaría de ciudad Nueva, Tacna 2021 [Universidad Privada de Tacna]. https://repositorio.upt.edu.pe/bitstream/handle/20.500.12969/2027/Cahuana-Caceres-Ccaso-Huacca.pdf?sequence=1&isAllowed=y*

Castañeda, A. E.; Mieles, Y. B. (2017). *Overview of the Structural Behavior of Columns, Beams, Floor Slabs and Buildings during the Earthquake of 2016 in Ecuador. Revista Ingeniería de construcción, 16.*

Cennamo, C.; Di Fiore, M. (2013). *Structural, seismic and geotechnical analysis of the Sant' Agostino church in L'aquila (Italy). Revista Ingeniería de Construcción, 14.*

Choque, J.; Luque, E. (2019). *Análisis estático no lineal y evaluación del desempeño sísmico de un edificio de 8 niveles diseñado con la norma E.030. Universidad Nacional de San Agustín de Arequipa.*

Condori, R.; Vilca, A. (2022). *Evaluación del desempeño estructural aplicando un análisis estático no lineal (Pushover) en la I. E. N.º 40230 San Antonio del Pedregal Majes - Caylloma - Arequipa. Universidad Continental.*

Cueva, C.; Huamanchumo, C. (2022). *Evaluación estructural de la edificación esencial I.E N°10133-Mochumí, mediante el análisis estático no lineal Pushover [Universidad Tecnológica del Perú]. https://repositorio.utp.edu.pe/bitstream/handle/20.500.12867/6187/C.Cueva_C.Huamanchumo_Tesis_Titulo_Profesional_2022.pdf?sequence=1&isAllowed=y*

Cumpa, J.; Quispe, B. (2019). *Evaluación del desempeño sismorresistente de la institución educativa n°50217 de la comunidad Umachurco-San Salvador, aplicando el método de análisis estático no lineal de cedencia sucesiva (Pushover) [Universidad Andina de Cusco]. https://repositorio.uandina.edu.pe/bitstream/handle/20.500.12557/2885/Brayan_Jinmy_Tesis_bachiller_2019_Part.1.pdf?sequence=1&isAllowed=y*

Díaz, D. A.; Diaz, S. A.; Pinzón, L. A.; H. J.; Mora Ortiz, R. S. (2022). *Seismic performance assessment based*

on the interstory drift of steel buildings. Latin American Journal of Solids and Structures, 18.

Edificaciones, R. N. (2018). *NORMA E.030 DISEÑO. Lima.*

Eduardo, D. (2019). *Verificación de la confiabilidad del análisis dinámico espectral mediante el análisis no lineal (Pushover) de un edificio de 5 niveles. Universidad Católica de Santa María.*

Etli, S.; Güneyisi, E. M. (2020). *Seismic performance evaluation of regular and irregular composite moment resisting frames. Latin American Journal of Solids and Structures, 22.*

FEMA. (2005). *HAZUS®MH MR4. Washington, D.C.*

Firoj, M.; Bahuguna, A.; Kanth, A.; Agrahari, R. (2022). *Effect of nonlinear soil− structure interaction and lateral stiffness on seismic performance of mid− rise RC building. ELSEVIER, 19.*

Gonzales, G.; Aguilar, A.; Huaco, G. (2020). *Incremental Dynamic Analysis of a 60 Year Old Hospital with Handmade Brick Masonry Walls. LACCEI, 7.*

Institution, B. S. (1988). *BS 1881-204:1988 (R2014). London.*

Jameel, M.; Islam, S.; Riswan Hussain, R.; Danish Hasan, S.; Khaleel, M. (2013). *Non-linear FEM Analysis of seismic induced pounding between neighbouring Multi-storey Structures. Latin American Journal of Solids and Structures, 19.*

Jinez, S.; Huarachi, D. (2023). *Análisis no lineal y evaluación de desempeño según ASCE/SEI 41 del pabellón "A" de la I.E. Jorge Chávez de la ciudad de Tacna, 2022 [Universidad Privada de Tacna]. https://repositorio.upt.edu.pe/bitstream/handle/20.500.12969/2977/Jinez-Mendoza-Huarachi-Quispe.pdf?sequence=1&isAllowed=y*

Lloclle, A. (2021). *Evaluación de desempeño estructural utilizando Análisis Estático no lineal (Pushover) del bloque del nivel secundario del colegio Emblemático Ladislao Espinar ubicado en la ciudad de Espinar – Cusco [Universidad Peruana Unión]. https://core.ac.uk/download/pdf/478791931.pdf*

Llontop, G. (2023). *Optimización del diseño estructural utilizando análisis estático no lineal Pushover en la I.E San Carlos-Monsefú [Universidad Católica Santo Toribio de Mogrovejo]. https://tesis.usat.edu.pe/bitstream/20.500.12423/6047/1/TL_LlontopMoraGreta.pdf*

Marín, W. (2020). *Nivel de desempeño sísmico de un edificio multifamiliar mediante el análisis estático no Lineal Pushover, Jesús María, 2020 [Universidad Cesar Vallejo].*

Murillo, M. (2022). *Determinación del nivel de vulnerabilidad sísmica en la ciudadela la Politécnica de la ciudad de Riobamba, aplicando el método de análisis lineal y no lineal Pushover. Universidad Internacional SEK.*

Núñez, F.; Ruiz, D.; Cortés, J. (2021). *Nonlinear dynamic analysis of steel buildings subjected to earthquakes. Revista Ingeniería de Construcción, 24.*

Peruana, N. T. (2011). *PNTP 339.059. Lima.*

Pimiento, J.; Ruiz, D.; Salas, A. (2014). *Seismic performance of frames with passive energy dissipation steel slit plates, 29(3). Revista Ingeniería de Construcción, 283-298. https://doi.org/10.4067/S0718-50732014000300005.*

Quinto, W.; Chaverra, E. (2022). *Análisis estático no lineal (Pushover) y punto de desempeño sísmico en una edificación de tres pisos existente – Revisión bibliográfica y caso ejemplo [Universidad de Antioquia]. https://bibliotecadigital.udea.edu.co/bitstream/10495/33261/4/QuintoWillman_2022_An%c3%a1lisis Pushover.pdf*

Sangucho, P. (2022). *Comparación de las filosofías de diseño y el desempeño real de una estructura, mediante análisis estático lineal, análisis Pushover y análisis de historia en el tiempo en una estructura de hormigón armado, incluyendo elementos no estructurales. Escuela Politécnica Nacional.*

Solorzano, J.; Tacuche, D. (2023). *Evaluación estructural mediante el análisis no lineal Pushover, para establecer el grado de vulnerabilidad sísmica que presenta el Centro de Salud Amarilis – Huánuco. Universidad Nacional Hermilio Valdizàn.*

STANDARD, A. (2017). *Seismic Evaluation and Retrofit of Existing Buildings. Virgina: SEI.*

Tagle, S. J., Junemann, R., Vasquez, J., Llera, J. C., & Baiguera, M. (2021). *Performance of a reinforced concrete wall building subjected to sequential earthquake and tsunami loading . ELSEVIER, 18.*

Tello, M.; Yacsavilca, E. (2023). *Análisis de la respuesta sísmica de un edificio de usos mixtos de 5 pisos de muros estructurales sin y con disipadores SLB en el distrito de San Juan de Miraflores - Lima [Universidad Tecnológica del Perú].*

https://repositorio.utp.edu.pe/bitstream/handle/20.500.12867/7273/M.Tello_E.Yacsavilca_Tesis_Titulo_Profesional_2023.pdf?sequence=1&isAllowed=y

Wang, H. f.; Zhang, R. l. (2021). *Dynamic structure-soil-structure interaction of piled high-rise buildings under earthquake excitations I: Influence on dynamic response . Latin American Journal of Solids ans Structures, 23*